

Lactosylated poly(ethylene oxide)–poly(propylene oxide) block copolymers for potential active targeting: synthesis and physicochemical and self-aggregation characterization

María L. Cuestas · Romina J. Glisoni ·
Verónica L. Mathet · Alejandro Sosnik

Received: 20 July 2012 / Accepted: 21 December 2012
© Springer Science+Business Media Dordrecht 2013

Abstract Aiming to develop polymeric self-assembly nanocarriers with potential applications in active drug targeting to the liver, linear and branched poly(ethylene oxide)–poly(propylene oxide) amphiphiles were conjugated to lactobionic acid (LA), a disaccharide of galactose and gluconic acid, by the conventional Steglich esterification reaction. The conjugation was confirmed by ATR/FT-IR, ¹H-NMR, and ¹³C-NMR spectroscopy. Elemental analysis and MALDI-TOF mass spectrometry were employed to elucidate the conjugation extent and the final molecular weight, respectively. The critical micellar concentration (CMC), the size and size distribution and zeta potential of the pristine and modified polymeric

micelles under different conditions of pH and temperature were characterized by dynamic light scattering (DLS). Conjugation with LA favored the micellization process, leading to a decrease of the CMC with respect to the pristine counterpart, this phenomenon being independent of the pH and the temperature. At 37 °C, micelles made of pristine copolymers showed a monomodal size distribution between 12.8 and 24.4 nm. Conversely, LA-conjugated micelles showed a bimodal size pattern that comprised a main fraction of relatively small size (11.6–22.2 nm) and a second one with remarkably larger sizes of up to 941.4 nm. The former corresponded to single micelles, while the latter would indicate a secondary aggregation phenomenon. The spherical morphology of LA-micelles was visualized by transmission electron microscopy (TEM). Finally, to assess the ability of the LA-conjugated micelles to interact with lectin-like receptors, samples were incubated with concanavalin A at 37 °C and the size and size distribution were monitored by DLS. Findings indicated that regardless of the relatively weak affinity of this vegetal lectin for galactose, micelles underwent agglutination probably through the interaction of a secondary site in the lectin with the gluconic acid unit of LA.

Keywords Poly(ethylene oxide)–poly(propylene oxide) polymeric micelles · Lactobionic acid-conjugated poloxamers and poloxamines · Steglich esterification · Concanavalin A agglutination

María L. Cuestas and Romina J. Glisoni equally contributed to this work.

M. L. Cuestas · R. J. Glisoni · A. Sosnik (✉)
The Group of Biomaterials and Nanotechnology for Improved Medicines (BIONIMED), Department of Pharmaceutical Technology, Faculty of Pharmacy and Biochemistry, University of Buenos Aires, 956 Junín St., 6th Floor, CP1113 Buenos Aires, Argentina
e-mail: alesosnik@gmail.com

M. L. Cuestas · R. J. Glisoni · V. L. Mathet · A. Sosnik
National Science Research Council (CONICET),
Buenos Aires, Argentina

V. L. Mathet
Department of Microbiology, Faculty of Medicine,
Center for the Study of Viral Hepatitis, University of
Buenos Aires, Buenos Aires, Argentina

Introduction

Persistent infections with the hepatitis B (HBV) and the hepatitis C virus (HCV) are associated with chronic hepatitis, cirrhosis, and the development of hepatocellular carcinoma (HCC) (Guidotti and Chisari 2006; El-Seraq and Rudolph 2007). The development of more effective antiviral agents appears as one of the most straightforward strategies to address the disease (Cuestas et al. 2010; Glisoni et al. 2010, 2012a, b). At the same time, the active targeting of drugs to the liver parenchyma might provide a unique window of opportunities to improve the efficacy of the pharmacotherapy, while reducing severe systemic side effects (Cuestas et al. 2010; Trevaskis et al. 2010).

Asialoglycoprotein receptors (ASGPRs) are glycoproteins located on the surface of the hepatocyte and intracellularly (50,000–500,000 per cell) (Eisenburg et al. 1991; Enrich et al. 1992). ASGPRs recognize serum asialoglycoproteins (ASGPs) through clustered galactose residues, removing them from the systemic circulation by endocytosis (Wu and Wu 1998; Tozawa et al. 2001).

The emergence of polymeric nanocarriers conjugated with specific ligands for the active targeting of drugs to diseased tissues and organs has revolutionized the pharmaceutical research (Gupta and Jain 2010). In the last two decades, several nanotechnologies have been explored to selectively deliver drugs to the hepatic parenchyma (De Paula et al. 2007; Feng et al. 2008; Kim et al. 2009; Wang et al. 2008; Weeke-Klimp et al. 2007; Mao et al. 2007; Nishina et al. 2008; Sato et al. 2008). Since ASGPRs are capable of importing large galactosylated structures across the cellular membrane and they are upregulated in some pathological conditions (e.g., HBV) (Yang et al. 2006), the design of galactose-decorated nanocarriers has come out as one of the most appealing approaches to improve the treatment of liver diseases (Eisenburg et al. 1991; Eto and Takahashi 1999; Li et al. 2008; Kikker et al. 2009; Zhang et al. 2011).

Polymeric micelles (PMs) are nanoscopic structures formed by the self-assembly of amphiphilic block copolymers above the critical micellar concentration (CMC) (Sosnik et al. 2008). PMs are composed of an inner hydrophobic core that can host hydrophobic drug molecules and an outer hydrophilic corona that physically stabilizes the aggregates in aqueous medium. This unique molecular arrangement makes

PMs appropriate for the encapsulation and/or the physicochemical stabilization of poorly water-soluble drugs. In addition, PMs have been used to passively target antitumoral drugs to highly vascularized solid tumors by the enhanced permeation and retention (EPR) effect (Alvarez-Lorenzo et al. 2010; Kim et al. 2004).

Poly(ethylene oxide)–poly(propylene oxide) (PEO–PPOs) block copolymers are among the most extensively investigated micelle-forming amphiphiles (Kataoka et al. 2001; Chiappetta and Sosnik 2007; Gonzalez-Lopez et al. 2008; Alvarez-Lorenzo et al. 2011). According to their molecular architecture, they are classified into two main groups: (i) the linear and bifunctional poloxamers (Pluronic[®]) and (ii) the four-arm poloxamines (Tetronic[®]) (Kataoka et al. 2001; Alvarez-Lorenzo et al. 2011). Poloxamers are thermo-responsive and their micellization is favored at higher temperatures. Conversely, poloxamines are dually responsive to temperature and pH owing to the presence of a central ethylenediamine moiety that undergoes protonation or deprotonation under acid and basic pH values, respectively (Fernandez-Tarrio et al. 2007; Alvarez-Lorenzo et al. 2011). The chemical structure of poloxamines can also be capitalized to chemically modify the micellar core (e.g., N-alkylation) (Sosnik and Sefton 2006) and to tune self-aggregation and drug encapsulation properties (Gonzalez-Lopez et al. 2008; Alvarez-Lorenzo et al. 2010; Chiappetta et al. 2010).

The goal of this study was to explore a technology platform for the potential targeting of hydrophobic drugs to the liver. In this context, we synthesized and fully characterized the physicochemical and self-aggregation properties of a series of lactosylated PEO–PPO copolymers displaying different molecular weights, hydrophilic–lipophilic balances and molecular architectures. Finally, the ability of the modified amphiphiles to bind a soluble vegetal lectin, namely Concanavalin A, was demonstrated.

Experimental section

Materials

Pluronic[®] F127 (F127, $M_w = 12,600$ g/mol; PEO weight content, % PEO = 70 %; hydrophilic–lipophilic balance, HLB = 18–23), Tetronic[®] 1107 (T1107, $M_w = 15,000$ g/mol, % PEO = 70 %, HLB =

18–23) and Tetronic[®] 904 (T904, $M_w = 6,700$ g/mol, % PEO = 40 %, HLB = 12–18) were a gift of BASF Corporation (New Milford, CT, USA). In the synthetic stages, copolymers were used without further purification, while in all the physicochemical and aggregation characterizations they were previously dialyzed against distilled water (regenerated cellulose dialysis membranes; molecular weight cut-off of 1,000 g/mol for T904 and 3,500 g/mol for F127 and T1107, respectively; Spectra/Por[®] 3 nominal flat width of 45 mm, diameter of 29 mm, and volume/length ratio of 6.4 mL/cm; Spectrum Laboratories, Inc., Rancho Dominguez, CA, USA) over 48 h and freeze-dried (see below). Lactobionic acid (4-*O*- β -galactopyranosyl-D-gluconic acid, LA; molar mass = 358.3 g/mol), *N,N'*-dicyclohexylcarbodiimide (DCC, carboxylic acid activator) and 4-dimethylaminopyridine (DMAP, acyl transfer agent) were purchased from Sigma-Aldrich Company (St. Louis, MO, USA) and used as received. All the solvents were of analytical or spectroscopic quality and used without further purification.

Synthesis of LA-conjugated block copolymers

The conjugation of LA to the terminal –OH of the corresponding PEO–PPO block copolymer was achieved by the conventional Steglich esterification reaction (Giacomelli et al. 2007). In brief, the copolymer (2.5–5 g), LA, DCC, and DMAP were dissolved separately in pure dimethylsulfoxide (DMSO, 10 mL) previously dried with molecular sieves 3A for at least 48 h (Sigma-Aldrich). Then, LA, DCC, and DMAP solutions were added successively to the corresponding copolymer solution under magnetic stirring. The reagent feeding ratios are summarized in Table 1. The reaction was allowed to proceed at room temperature (72 h) under magnetic stirring and the resulting solution was diluted in water (1:2) and dialyzed against water for 4 days with

frequent exchanges of the dialysis medium. Solutions were filtered by filter paper (Filter Discs Qual., Grade 289, Sartorius AG, Goettingen, Germany), frozen at -20 °C (24 h) and freeze-dried (Lyophilizer L05, F.i.c. Scientific Instrumental Manufacturing, Buenos Aires, Argentina) at a condenser temperature of -45 °C and 30 μ bar pressure during 48 h. Products were stored at -20 °C until use. The modified copolymers of F127, T1107, and T904 are named F127-LA, T1107-LA, and T904-LA, respectively, independently of the LA conjugation extent (see below).

Characterization of pristine and LA-conjugated block copolymers

Attenuated total reflectance/Fourier transform-infrared spectroscopy (ATR/FT-IR)

The modification of the different copolymers with LA was characterized by ATR/FT-IR spectroscopy (Nicolet 380 ATR/FT-IR spectrometer, Avatar Combination Kit, Smart Multi-Bounce HATR with ZnSe crystal 45° reflectance, Thermo Scientific, Madison, WI, USA) in the range between 4,000 and 600 cm^{-1} (32 scans, spectral resolution of 4 cm^{-1}). Pure LA and pristine copolymers were used as controls. Solid samples were mounted on the ATR crystal-metal plate and spectra were obtained using the OMNIC 8 spectrum software (Thermo Scientific).

Nuclear magnetic resonance (NMR) analysis

To confirm the conjugation of the LA moiety, ¹H-NMR and ¹³C-NMR spectra of the different pristine and LA-modified copolymers were recorded using a Bruker[®] Avance II High-Resolution 500-MHz multi-nuclear spectrometer and Bruker TOPSPIN 2.1 software (Bruker BioSpin GmbH, Rheinstetten, Germany)

Table 1 Reagent feeding ratios used for the conjugation of LA to PEO–PPO block copolymers by the Steglich esterification reaction

Pristine copolymer	Number of terminal –OH groups/mol	Copolymer weight (g) ^a	M_w (g/mol)	Reagent feeding ratio (mg)			Yield (%)	Elemental analysis	
				LA ^a	DCC ^a	DMAP ^a		#LA	DLAS (%)
F127	2	5	12,600	284	330	39	65	1	50
T1107	4	2.5	15,000	275	325	38	65	1	25
T904	4	2.5	6700	550	650	75	45	3	75

^a Each reagent was separately dissolved in 10 mL of dry DMSO

in deuterated dimethylsulfoxide (DMSO- d_6) with tetramethylsilane as internal standard at 298 K. The accumulation time for ^{13}C -NMR analysis was 2.3 h.

Elemental analysis

The elemental composition (%) of pristine and LA-modified copolymers was determined by elemental analysis (Carlo Erba 1108 CHNS analyzer, Carlo Erba, Milan, Italy). To determine the degree of LA substitution (DLAS) of each LA-conjugated copolymer, the experimental ratio between the percentage composition of carbon (%[C]) and oxygen (%[O]) was calculated and compared to the theoretical ratio obtained when considering substitution extents of 25, 50, 75, and 100 % for T1107 and T904 and 50 and 100 % for F127. Poloxamines display four –OH groups, thus these substitution percentages corresponded to 1, 2, 3, and 4 LA moieties per copolymer molecule. The bifunctional poloxamers could only bear 1 or 2 LA substituents. Thus, the experimental conjugation extent was estimated by comparing the experimental elemental composition of the each lactosylated derivative with the theoretical one for each theoretical conjugate bearing a growing number of LA residues. This data were complemented with matrix-assisted laser desorption/ionization time of flight mass spectrometry analysis (see below).

Matrix-assisted laser desorption/ionization time of flight mass spectrometry (MALDI-TOF MS)

The molecular weight of pristine and modified copolymers was determined by MALDI-TOF MS (AUTOFLEX[®] mass spectrometer, Bruker Daltonics Inc., Billerica, MA, USA) equipped with a pulsed nitrogen laser, operating at a wavelength of 337 nm in linear and reflectron mode, extracting positive ions with an accelerating voltage of 25,000 V, grid voltage set and grid wire voltage of 95 and 0.005 %, respectively, and a delay time of 350 ns. The detection system consisted of a Micro Plate Channel with high sensitivity and dynamic range. 2-(4-Hydroxyphenylazo)-benzoic acid (0.1 M in chloroform) was a suitable matrix for these copolymers. Samples were prepared following a technique previously reported (Gallet et al. 2002). Copolymers were initially dissolved in chloroform (5 mg/mL) and NaCl solution (0.1 M in water, 1 μL) was added to aid cationization (sample

solution). Sample and matrix solutions were mixed in a 1:1 (v/v) ratio, deposited (1 μL) onto the MALDI sample holder and slowly dried to allow matrix crystallization. MALDI-TOF MS spectra were recorded in the m/z range between 2000 and 20,000 g/mol and represented as the intensity as a function of $[m/z + \text{Na}]^+$ in g/mol (Bruker Daltonics flex Analysis software, Bruker Daltonics Inc.).

Thermal analysis

The thermal behavior of the different pristine and modified copolymers was analyzed by differential scanning calorimetry (DSC) using a Q100 V9.5 Build 288 differential scanning calorimeter (Universal V4.2E TA Instruments, New Castle, DE, USA) fitted with a liquid nitrogen cooling system. Dry samples (2–8 mg) were sealed in 40 μL Al-crucible pans and subjected to three consecutive thermal treatments at a heating/cooling rate of 5 $^\circ\text{C min}^{-1}$ and under nitrogen atmosphere: (i) heating from 25 to 100 $^\circ\text{C}$ (first heating ramp), (ii) cooling from 100 to –30 $^\circ\text{C}$ (cooling ramp), and (iii) heating from –30 to 150 $^\circ\text{C}$ (second heating ramp). The crystallization (T_c) and the melting temperature (T_m) of PEO blocks and the enthalpy involved in each transition, ΔH_c and ΔH_m , were calculated from the exothermic and endothermic peaks, respectively, registered during the cooling and the second heating ramps (see above). The relative tendency of the different pristine and modified copolymers to crystallize was estimated by the difference between T_m and T_c , ΔT , according to Eq. 1

$$\Delta T = T_m - T_c. \quad (1)$$

Determination of the CMC

CMC values of F127, T1107, T904 and their LA-conjugated counterparts were determined in water (Simplicity[®] Water Purification System, Millipore, Billerica, MA, USA; pH 5.8) and phosphate buffered saline (PBS, pH 7.2, GIBCO[®] Phosphate-Buffered Saline 7.2, Life Technologies Corp., Carlsbad, CA, USA) at 25 and 37 $^\circ\text{C}$. Derived Count Rate (DCR) measurements were carried out by means of dynamic light scattering (DLS, Zetasizer Nano-ZS, Malvern Instruments, Worcestershire, UK) at scattering angle of 173 $^\circ$ (Chiappetta et al. 2011; Glisoni et al. 2012a). The Nano-ZS contains a 4-mW He–Ne laser operating at a wavelength of 633 nm, a digital correlator ZEN3600,

and a Non-Invasive Back Scatter (NIBS[®]) technology. For the measurements, PEO–PPO block copolymers were solubilized (5 % w/v final concentration) in water or PBS at 4 °C, the solutions were filtered (0.22 µm, GE nitrocellulose mixed esters membrane, Osmonics Inc., Minnesota, MN, USA) and finally diluted to the final concentration (0.00125–5 % w/v) with the corresponding medium. Then, samples were equilibrated at the corresponding temperature for at least 24 h and analyzed by DLS. The intensity of the scattered light (DCR) expressed in kilo counts per second (kcps) was plotted as a function of the copolymer concentration (% w/v) (Chiappetta et al. 2011; Glisoni et al. 2012a). Data for each single specimen were the result of five runs. The micellization was observed as a sharp increase in the scattering intensity. The intersection between the two straight lines corresponded to the CMC (Chiappetta et al. 2011; Glisoni et al. 2012a).

Size, size distribution, and Z-potential (Z-pot) analysis

The hydrodynamic diameter (D_h) and the size distribution (polydispersity index, PDI) of freshly prepared pristine and LA-conjugated micelles (5 % w/v final concentration) prepared in water and PBS were measured by DLS (see above) at 25 and 37 °C. Z-pot of the different samples were also assayed by DLS. Refractive indices used for these measurements were between 1.333 and 1.345. Viscosities ranged between 0.8868 and 0.8898 cP at 25 °C and 0.6852–0.6870 cP at 37 °C. Results are expressed as mean \pm SD of three independent samples prepared under identical conditions. Data for each single specimen were the result of at least six runs.

Transmission electron microscopy (TEM) analysis

The morphology of T904 and T904-LA micelles was visualized using a Philips EM 301 transmission electron microscope (Zeiss, Eindhoven, The Netherlands) operating at an acceleration voltage of 60,000 V. Samples in water (5 % w/v, 20 µL) properly stabilized at 37 °C for 30 min prior to the analysis were deposited onto Formvar carbon-coated copper grids. After soaking the excess of sample with filter paper, the grid was covered with a drop of uranyl acetate solution (5 µL, 2 % w/v, negative staining method) during 60 s. Then, grids were air-dried and analyzed.

Agglutination of LA-conjugated block copolymers

The agglutination of LA-conjugated copolymers in the presence of the vegetal lectin Concanavalin A (Con A, from *Canavalia ensiformis*, Jack Bean Type VI, lyophilized powder, Sigma-Aldrich) was assessed by DLS as described elsewhere with slight modifications (Vetri et al. 2010; Wang et al. 2011). Briefly, micelle samples (10 % w/v PBS, pH 7.2, 500 µL) containing bovine serum albumin (BSA, 6 % w/v, Type V, Sigma-Aldrich) were incubated for 30 min at room temperature, under continuous stirring. Then, Con A stock PBS solution (1.0 mg/mL) was added (500 µL) to the micelles. The final concentrations of the copolymer, BSA and Con A in the sample were 5 % w/v, 3 % w/v, and 0.5 mg/mL, respectively. Samples were incubated under moderate stirring at 37 °C for 2 h and the D_h and the PDI monitored by DLS. The following controls were analyzed: (i) BSA 3 % w/v in PBS, (ii) BSA 3 % w/v/Con A (0.5 mg/mL final concentration) in PBS, and (iii) pristine copolymers (5 % w/v final concentration) in BSA 3 % w/v/Con A (0.5 mg/mL) in PBS. Results are expressed as mean \pm SD of three independent samples prepared under identical conditions. Data for each single specimen were the result of at least six runs.

Data analysis

The statistical analysis was performed by a one-way ANOVA (5 % significance level, P values >0.05 were considered statistically significant) combined with the Dunnett Multiple Comparison Test or t test (5 % significance level, P values >0.05 were considered statistically significant). The software used was GraphPad Prism version 5.00 for Windows (GraphPad Software Inc., San Diego, CA, USA).

Results

Synthesis of LA-conjugated block copolymers

LA is a disaccharide produced by the oxidation of lactose that has been used as a recognition moiety for the targeting of drug carriers to the hepatocyte (Fiume et al. 1994; Gao et al. 2003; Wang et al. 2006). The conjugation of LA to the terminal –OH groups of linear and branched PEO–PPO copolymers

Characterization of pristine and LA-conjugated block copolymers

The LA-functionalized block copolymers were extensively characterized by different techniques.

ATR/FT-IR

The spectrum of pure LA showed the band corresponding to the stretching vibration of the carbonyl group at 1737 cm^{-1} (Fig. 2A). Pristine copolymers showed the C–H and C–O–C stretching vibrations of PEO and PPO at $2970\text{--}2874$ and $1080\text{--}1104\text{ cm}^{-1}$, respectively (Fig. 2B). These bands were also apparent in the LA-modified derivatives (Fig. 2C). In addition, F127-LA, T1107-LA, and T904-LA displayed the distinctive carbonyl band of LA at 1740 , 1729 , and 1735 cm^{-1} , respectively (Fig. 2C); this band being absent in the spectrum of the pristine counterparts. Finally, the intensity of –OH bands at $3350\text{--}3494\text{ cm}^{-1}$ did not change upon LA conjugation.

NMR analysis

The structure of the different pristine and LA-modified copolymers was further characterized by ^1H -NMR and ^{13}C -NMR. The protons of PPO ($-\text{CH}_3$) and PEO ($-\text{CH}_2-\text{CH}_2-$) were observed at $1.13\text{--}1.15$ and $1.04\text{--}1.12$ ppm and $3.53\text{--}3.73$ and $3.50\text{--}3.63$ ppm for the pristine and the modified copolymers, respectively (Fig. 3). In addition, in the LA-conjugated derivatives, the protons of the sugar residue were apparent at lower fields, between 4.18 and 5.26 ppm (Fig. 3, inset).

^{13}C -NMR spectra showed the characteristic signals of the polymeric carbons in the range between 10 and 86 ppm (Fig. 4). In addition, LA-modified derivatives showed the distinctive signals of carbonyl groups of LA at $170.97\text{--}171.50$ ppm (Fig. 4B, inset), confirming the conjugation. On the other hand, it is important to mention that the signal at 103.93 ppm (Fig. 4B, inset) was characteristic of the anomeric carbon of the galactose residue, while the other carbons of the LA moiety were probably apparent between 60 and 80 ppm (Fig. 4B, inset), as reported elsewhere for LA–poly(amido-amine) conjugates (Casali et al. 2001).

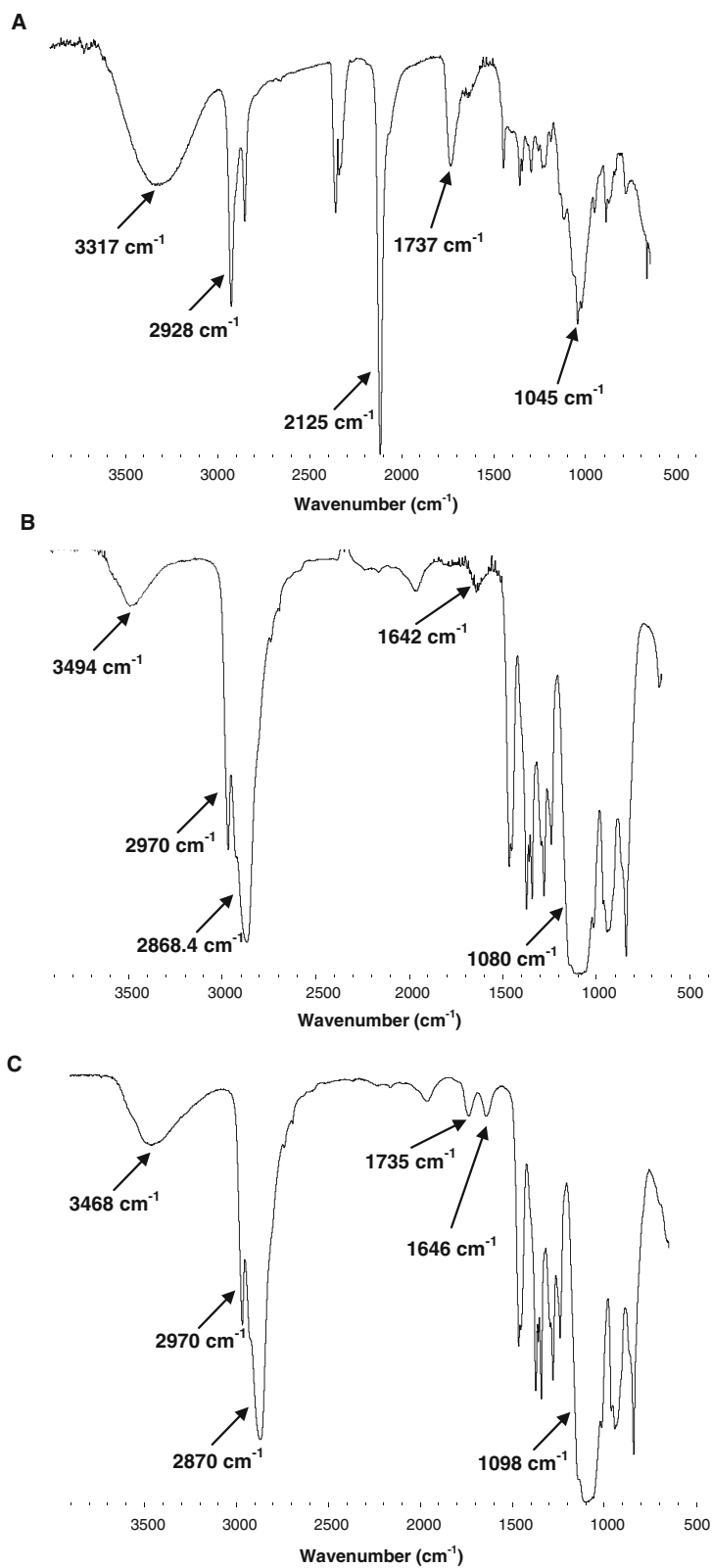
Elemental analysis

To estimate the number of LA units (#LA) per F127, T1107, and T904 molecule, the elemental composition of the different pristine and modified copolymers was determined by elemental analysis. Experimental results were compared to the theoretical elemental composition of LA-modified counterparts with substitution extents of 50 and 100% for F127 and 25 , 50 , 75 , and 100% for both poloxamines (Table 2). These extents were equivalent to 1 and 2 LA groups per bifunctional poloxamer and 1 , 2 , 3 , and 4 per tetrafunctional poloxamine. F127-LA and T1107-LA data were in agreement with DLAS of 50 and 25% , respectively (Table 1). Conversely, T904-LA showed a greater DLAS of 75% (3 LA molecules were conjugated with one copolymer molecule) (Table 1).

MALDI-TOF MS

Figure 5 shows MALDI-TOF MS spectra of F127, T1107, and T904 and their corresponding LA-conjugated counterparts. Maximum intensity peaks appear as $[m/z + \text{Na}]^+$ (expressed in g/mol) due to the formation of Na alkoxides in the respective terminal groups of fragmented PEO–PPO copolymers. All the derivatives displayed a bimodal distribution (Fig. 5). The distribution of F127 ranged from 2370.3 to 6863.6 g/mol, with two maxima at m/z 3472.4 and 4950.0 g/mol (Table 3). Pristine T1107 and T904 showed a similar behavior; the smaller molecular weight maximum being at 3824.9 g/mol (range between 2237.9 and 4658.7 g/mol) and 3509.9 g/mol (range between 2616.9 and 4367.6 g/mol), respectively (Table 3; Fig. 5). In addition, the greater molecular weight fraction was at 7787.6 g/mol (range between 7451.1 and 8034.3 g/mol) for T1107 and 7112.3 g/mol (range between 6408.8 and 7832.8 g/mol) for T904. The distribution of F127-LA was similar to that of the unmodified copolymer, m/z ranging between 2194.5 and 6158.5 g/mol with two maxima at 3517.2 and 5013.5 g/mol (Table 3; Fig. 5). In addition, a slight increase of m/z was observed in both fractions. T1107-LA and T904-LA followed a similar trend. For example, T1107-LA showed two m/z distributions at (i) $2442.7\text{--}4922.5$ g/mol and (ii) $7497.5\text{--}8750.0$ g/mol that corresponded to two maxima at 3827.1 and 7802.6 g/mol, respectively (Table 3; Fig. 5). Thus, the mean molecular

Fig. 2 ATR/FT-IR spectra of **A** LA, **B** pristine T904, and **C** T904-LA. Pristine T904 was dialyzed and lyophilized before the analysis



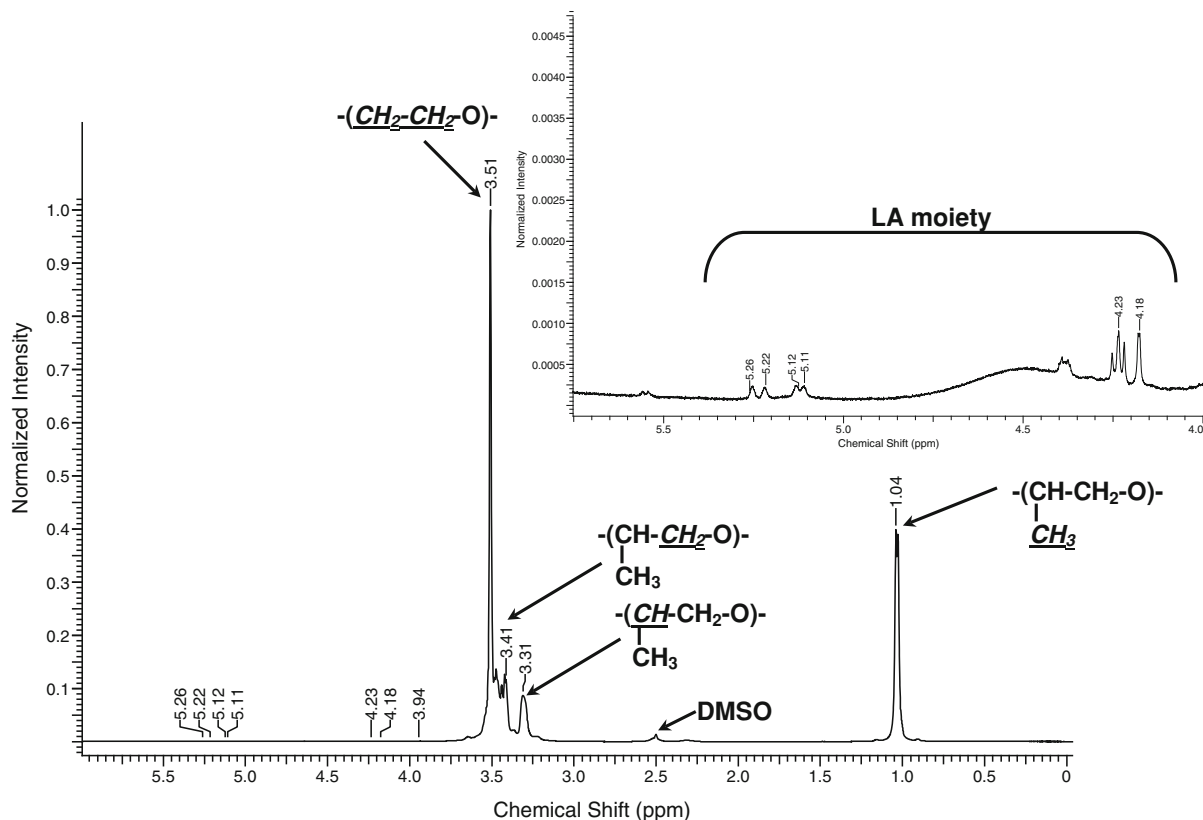


Fig. 3 ¹H-NMR spectrum of T904-LA in DMSO-*d*₆. The inset shows the characteristic signals of LA between 4.18 and 5.26 ppm

weight of the pristine F127, T1107, and T904 by MALDI-TOF MS were 12,265.0, 15,399.2, and 7024.3 g/mol, respectively. As expected, LA-modified derivatives showed a slight increase of the molecular weight in the different fractions due to the conjugation of LA residues (Table 3). In addition, the differences found in the molecular weight between pristine and modified copolymers were in the range of the molecular weight of the LA unit (Table 3).

Thermal behavior

Aiming to elucidate the effect of LA conjugation on the crystallization and melting of PEO blocks, the thermal properties of the different copolymers were studied by DSC; PPO segments are 100 % amorphous. Samples were initially heated from room temperature to 100 °C to erase the thermal history and then they were exposed to a cooling/heating cycle. The *T_c* was evidenced as a sharp exothermic peak at 31.2, 26.7, and 4.2 °C for pristine F127, T1107, and T904,

respectively (Table 4; Fig. 6). Conjugation of LA residues led to slight increase of 3.5 °C in the *T_c* of F127 to 34.7 °C for F127-LA. T1107 followed a similar trend with an increase of 1.5 to 28.2 °C for T1107-LA, while it decreased the *T_c* of T904 in 14.7 to −10.5 °C for T904-LA (Table 4; Fig. 6). The *T_m* was visualized as broad endothermic peak during the second heating ramp. Pristine F127, T1107, and T904 showed this transition at 54.7, 48.9, and 26.7 °C, respectively. F127-LA showed a slightly higher *T_m* at 55.1 °C, while T1107-LA and T904-LA exhibited slightly lower *T_m*, values being 48.5 and 24.3 °C, respectively. ΔH_c and ΔH_m were independent of the lactosylation and pristine and modified copolymers showed similar values; in all the cases, the enthalpy involved in the crystallization and melting were almost identical.

ΔT was calculated to estimate the tendency of PEO segments to crystallize; the greater the ΔT , the smaller the crystallization tendency and the greater the deleterious effect of conjugated LA residues. F127-LA

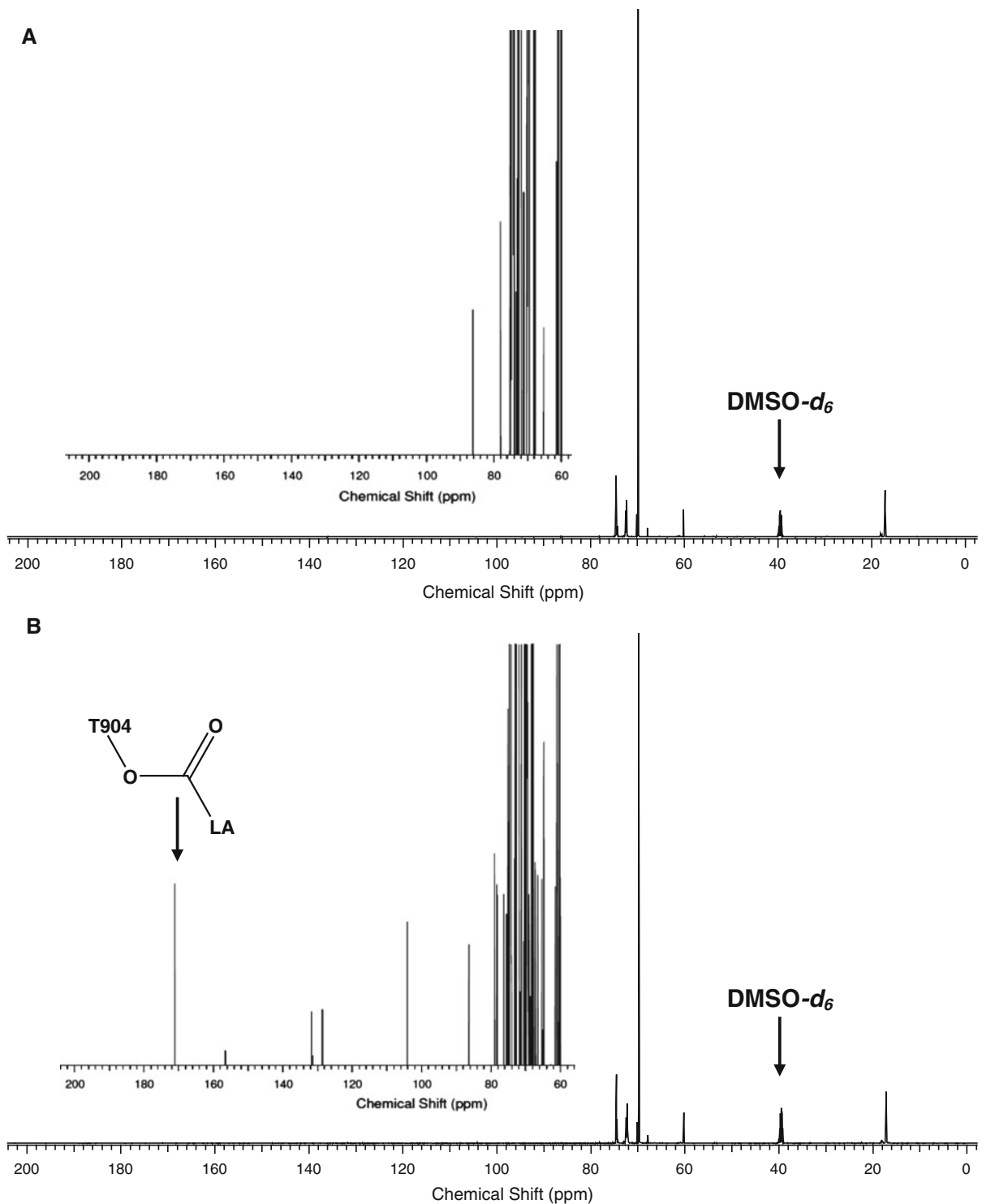


Fig. 4 ¹³C-NMR spectra of **A** pristine T904 and **B** T904-LA in DMSO- d_6 . *Inset* shows the magnification of the spectrum between 60 and 200 ppm. The characteristic signal of the newly

formed ester bond at 170.97 ppm is indicated in **(B)** with an *arrow*. The pristine copolymer was dialyzed and lyophilized before the analysis

Table 2 Theoretical and experimental elemental compositions of pristine and LA-conjugated PEO-PPO block copolymers

Copolymer	Calculation	Elemental composition				
		%[C]	%[O]	%[N]	%[H]	%[C]/%[O]
F127	Experimental	54.0	35.4	0	10.6	1.5
F127-LA		56.6	33.6	0	9.8	1.7
F127-LA ₁	Theoretical	56.4	34.2	0	9.4	1.7
F127-LA ₂		56.0	34.7	0	9.3	1.6
T1107	Experimental	56.7	32.5	0.2	10.6	1.7
T1107-LA		56.0	33.0	0.2	10.8	1.7
T1107-LA ₁	Theoretical	56.5	33.9	0.2	9.4	1.7
T1107-LA ₂		56.2	34.3	0.2	9.3	1.6
T1107-LA ₃		55.8	34.7	0.2	9.3	1.6
T1107-LA ₄		55.6	35.0	0.2	9.2	1.6
T904	Experimental	58.8	30.7	0.5	10.0	1.9
T904-LA		56.3	32.9	0.5	10.3	1.7
T904-LA ₁	Theoretical	58.1	31.9	0.4	9.6	1.8
T904-LA ₂		57.3	32.8	0.4	9.5	1.8
T904-LA ₃		56.7	33.6	0.4	9.3	1.7
T904-LA ₄		56.0	34.4	0.4	9.2	1.6

The %[C]/%[O] ratio was used to estimate the degree of LA substitution in each block copolymer

and T1107-LA showed ΔT of 20.4 and 20.3 °C, respectively, these values being slightly lower than those of the unmodified counterparts. Conversely, T904-LA displayed a sharp increase of ΔT to 34.8 °C (Table 4; Fig. 6).

Self-aggregation properties

The goal of the LA conjugation was to enable the active targeting of an encapsulated drug to specific cell types (e.g., hepatocyte). However, LA-conjugated amphiphiles could display different micellization behaviors than that of the pristine derivative. In this framework, characterizing their self-aggregation properties was of special interest. In water (pH 5.8) at 25 °C, pristine F127, T1107, and T904 showed CMC values of 0.250, 0.300, and 0.440 % w/v (Table 5). The increase of the temperature resulted in a slight to sharp decrease of the CMC; e.g., the CMC of F127 being 0.06 % w/v at 37 °C. In PBS, F127 showed CMC of 0.562 % w/v (25 °C) and 0.270 % w/v (37 °C), these values being greater than those determined in water. Conversely, T1107 and T904 showed a CMC decrease, this phenomenon being especially remarkable for T1107. All the modified amphiphiles showed CMC values that were smaller than those of the pristine counterpart under the same conditions (Table 5).

DLS was also employed to compare (i) the hydrodynamic diameter (D_h) and size polydispersity and (ii) the surface charge density of F127-LA, T1107-LA, and T904-LA micelles with respect to the unmodified copolymers. In general, at 25 °C, 5 % w/v systems in water displayed two size populations: (i) a small size fraction (5.0–22.2 nm) and (ii) a large size fraction ranging between 53.2 and 355.3 nm (Table 6). LA-modified copolymers led to larger aggregates, this behavior being more pronounced for poloxamines. The properties of the micelles were markedly different at 37 °C. Pristine copolymers showed a monomodal size distribution of small PMs with sizes between 12.8 and 24.4 nm (Table 6). This aggregation pattern was consistent with a more complete micellization. Conversely, in LA-conjugated copolymers, two size populations were still apparent: one of them being almost identical to that of the unmodified derivatives (11.6–22.2 nm) and a second population of substantially larger size in the range between 147.8 and 941.4 nm (Table 6). In addition, the contribution of this new size population increased from 11.1 % for F127-LA to 29.9 % for T1107-LA, and to 37.0 % for T904-LA. A similar trend was observed in PBS (data not shown).

In water at 25 °C, F127, T1107, and T904 micelles showed Z-pot values of -4.01, -9.93, and -6.91 mV, respectively. A slight increase of the Z-pot (and the

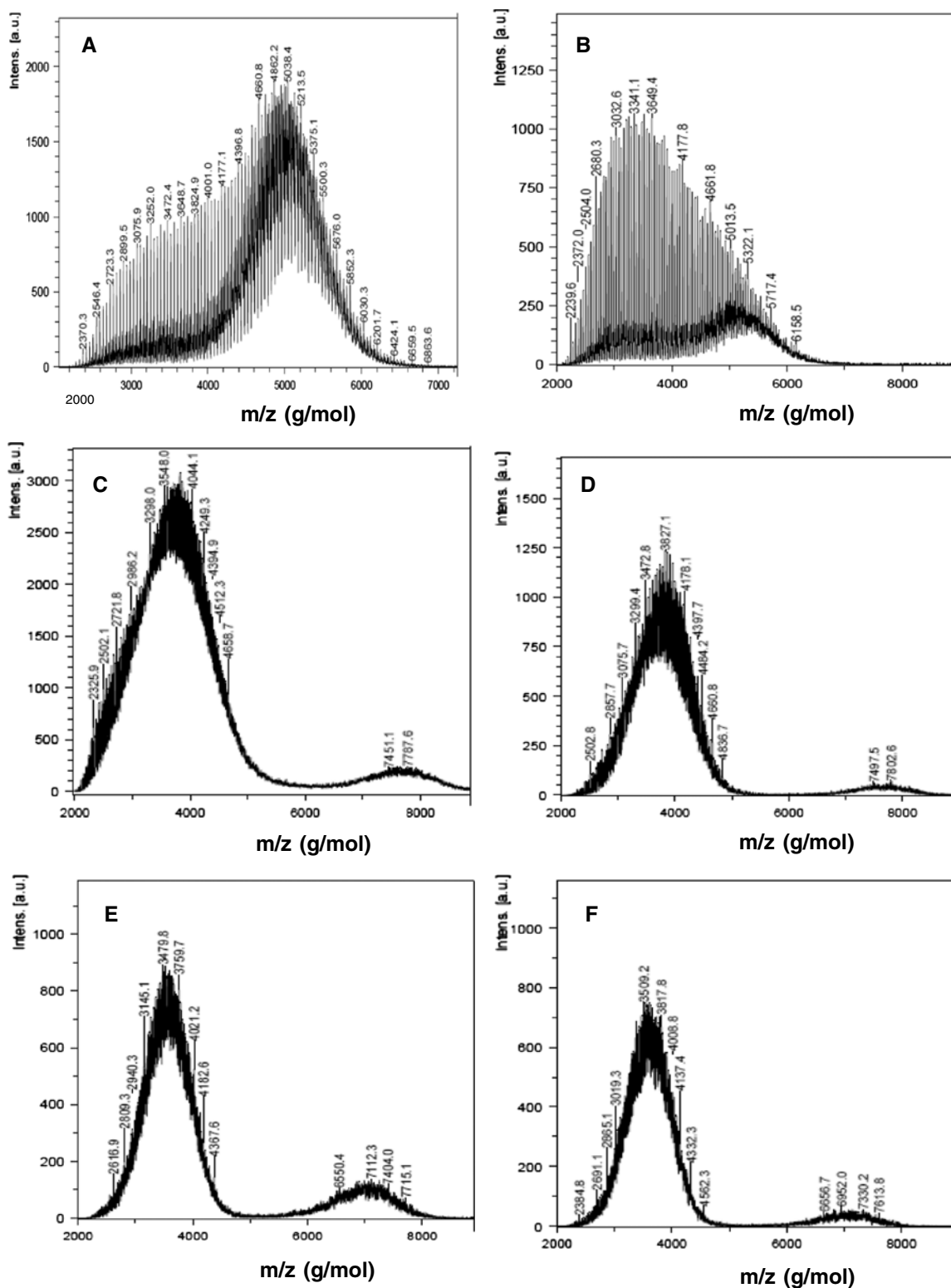


Fig. 5 Representative MALDI-TOF spectra of pristine and modified PEO-PPO block copolymers. **A** pristine F127, **B** F127-LA, **C** pristine T1107, **D** T1107-LA, **E** pristine T904, and **F** T904-LA. Pristine copolymers were dialyzed and lyophilized before the analysis

Table 3 Mean weight molecular mass (M_w) fractions of pristine and LA-conjugated block copolymers as determined by MALDI-TOF MS

Copolymer	$[m/z + Na]_1$ (g/mol)	$[m/z + Na]_2$ (g/mol)	Experimental molecular weight (g/mol) ^a
F127	3472.4	4950.0	12,265.0
F127-LA	3517.2	5013.5	12,478.8
T1107	3824.9	7787.6	15,399.2
T1107-LA	3827.1	7802.6	15,473.2
T904	3509.9	7112.3	7024.3
T904-LA	3817.8	7330.2	7308.2

^a Values of experimental molecular weight were calculated after the subtraction of 23 g/mol corresponding to the weight of Na^+

Table 4 DSC data of the different pristine and LA-conjugated block copolymers

Copolymer	T_c^a (°C)	ΔH_c^a (J/g)	T_m^b (°C)	ΔH_m^b (J/g)	ΔT^c (°C)
F127	31.2	133.8	54.7	134.6	23.5
F127-LA	34.7	135.3	55.1	134.7	20.4
T1107	26.7	123.1	48.9	124.8	22.2
T1107-LA	28.2	120.9	48.5	119.1	20.3
T904	4.2	59.2	26.7	57.8	22.5
T904-LA	-10.5	57.0	24.3	55.3	34.8

^a Determined during the cooling ramp

^b Determined during the second heating ramp

^c ($T_m - T_c$)

electrophoretic mobility) to less negative values was evident after the modification of the copolymers with LA (Table 6); the lactosylated counterparts remained negatively charged though values were -1.91 mV (F127-LA), -5.78 mV (T1107-LA), and -5.92 mV (T904-LA). Heating of the systems to 37 °C generally resulted in a change of the Z-pot to less negative values (Table 6).

Morphology

The spherical morphology of pristine and modified micelles was confirmed by TEM, as exemplified for T904 and T904-LA micelles (Fig. 7). The size and size distribution fitted well with DLS data (Table 6).

Agglutination of LA-conjugated block copolymers with Con A

The availability of sugar molecules on the surface of the PMs is a prerequisite to enable their interaction with the lectin receptors and the active targeting of the encapsulated drug to a specific cell type. To preliminarily assess the effect of the lactosylation on the interaction of the micelles with lectins, the different pristine and LA-modified PMs were incubated with a soluble vegetal lectin, Con A and the D_h and the PDI were monitored over 2 h by DLS (Vetri et al. 2010; Wang et al. 2011). Pristine F127, T1107, and T904 micelles showed some unspecific aggregation with size growths from 167.0, 225.9, and 207.2 nm to 348.8, 379.2, and 317.0 nm, respectively (Table 7). Concomitantly, PDI values increased from 0.30–0.36 to 0.50–0.90. The agglutination of LA-conjugated micelles led to more substantial size increments; sizes were 479.2, 511.4, and 503.5 nm for F127-LA, T1107-LA, and T904-LA agglutinates, respectively. In the exclusive case of LA-conjugated derivatives, this phenomenon was accompanied with a more pronounced increase of the % of the larger size population (73.2–87.7 %).

Discussion

Previous studies supported that the targeted delivery of antiviral and antitumoral drugs to the liver potentially increases the efficacy of these agents in the treatment of viral liver infections and HCC. At the same time, the more limited systemic exposure decreases their toxic effects in other tissues and organs. In this framework, the implementation of liver-targeting drug delivery systems and, in particular, nanotechnology strategies may provide tools to (i) improve the effectiveness and applicability of already approved and new drugs by overcoming or delaying the development of viral and cellular resistance, (ii) constrain the appearance of systemic side effects by promoting selective accumulation in the liver, and (iii) increase patient compliance by increasing the accumulation in the target-organ and reducing the administration frequency (Cuestas et al. 2010).

Aiming to introduce targeting properties to PEO–PPO micelles of different architectures, in this study, LA was conjugated to the terminal groups of the linear

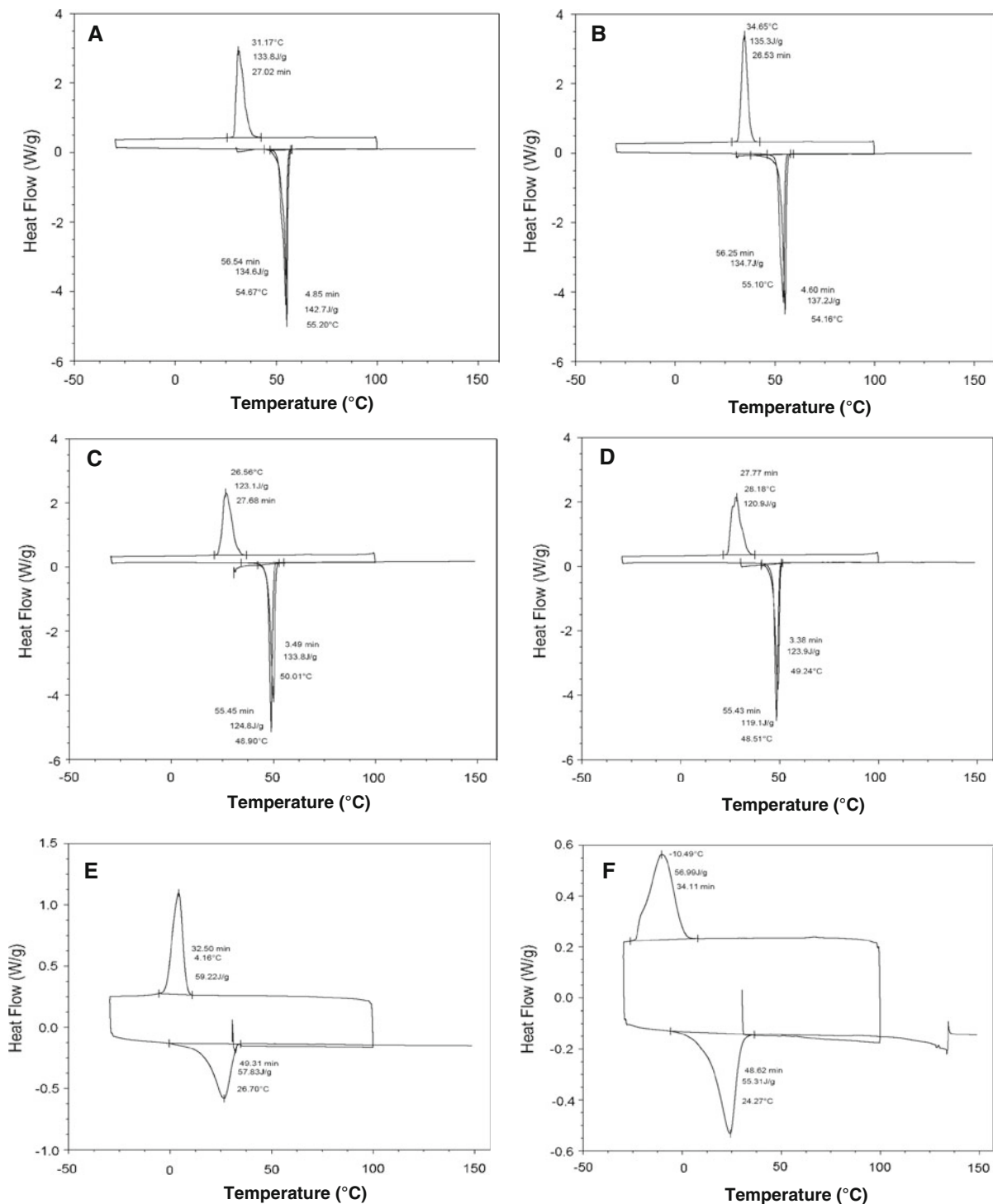


Fig. 6 Representative DSC of pristine and modified PEO-PPO block copolymers. **A** Pristine F127, **B** F127-LA, **C** pristine T1107, **D** T1107-LA, **E** pristine T904, and **F** T904-LA. Pristine copolymers were dialyzed and lyophilized before the analysis

Table 5 Experimental CMC values of the different pristine and LA-conjugated block copolymers in water and PBS at 25 and 37 °C, as determined by DLS

Copolymer	Water (% w/v)		PBS (% w/v)	
	25 °C	37 °C	25 °C	37 °C
F127	0.250	0.060	0.562	0.270
F127-LA	0.220	0.044	0.250	0.120
T1107	0.300	0.290	0.140	0.120
T1107-LA	0.100	0.150	0.090	0.110
T904	0.440	0.350	0.350	0.320
T904-LA	0.430	0.075	0.290	0.030

and branched copolymers employing a straightforward synthetic pathway. The conjugation of LA was confirmed by ATR/FT-IR and ¹H-NMR due to the appearance of the characteristic signals of the sugar. A priori, a decrease of the –OH band intensity in ATR/FT-IR (3400–3500 cm⁻¹) due to the esterification could be expected. However, the incorporated substituent displays a quite large amount of aliphatic –OH functional groups that compensated the intensity decrease of the polymeric hydroxyl moieties. Therefore, pristine and modified copolymers showed similar signal intensities in this region of the spectrum. Moreover, ¹H-NMR and ¹³C-NMR spectra showed

the characteristic signals of –OH groups of LA at 4.18–5.26 ppm (Fig. 3) and of C=O groups of the ester bond at 170.97 ppm (Fig. 4b, inset), respectively.

To establish the LA degree of substitution, the elemental composition of the conjugates was determined by elemental analysis and the results compared to the composition of copolymers bearing growing theoretical conjugation extents. Results indicated that F127-LA and T1107-LA contained one single LA residue, representing a DLAS of 50 and 25 %, respectively. A more efficient conjugation of LA was observed for T904, the copolymer with the lowest average molecular weight and the greatest HLB.

MALDI-TOF MS is a soft ionization technique that allows the analysis of intact high mass molecules such as proteins, glycoproteins, oligosaccharides, and other biopolymers because it prevents profuse fragmentation, a phenomenon that makes data evaluation very difficult (Li et al. 2010). Thus, this technique was an excellent tool for the elucidation of the structure and the molecular weight of polyethoxylated multicomponent mixtures (Gallet et al. 2002; Raith et al. 2006). In the positive mode, instead of protonation, polyethoxylates such as PEO–PPOs are ionized by the formation of adducts with ions of alkaline metals, mostly Na⁺ or K⁺, which can lead to different homologous series of $[m/z + Na]^+$ and $[m/z + K]^+$, respectively (Bootz

Table 6 Size (D_h), size distribution (PDI), Z-pot and electrophoretic mobility of 5 % (w/v) pristine and LA-conjugated PEO–PPO block copolymer micelles in water at 25 and 37 °C, as measured by DLS

Copolymer	T (°C)	Peak 1 ^a		Peak 2 ^b		PDI (±SD)	Z-pot (mV) (±SD)	Electrophoretic mobility (μm cm/Vs) (±SD)
		D_h (nm) (±SD)	% Intensity (±SD)	D_h (nm) (±SD)	% Intensity (±SD)			
F127	25	5.4 (0.2)	8.5 (4.0)	53.2 (2.3)	91.5 (4.0)	0.36 (0.04)	–4.01 (1.19)	–0.284 (0.111)
F127-LA		22.2 (1.7)	87.1 (4.4)	221.4 (39.3)	12.9 (4.4)	0.32 (0.02)	–1.91 (0.18)	–0.149 (0.014)
T1107		5.3 (0.2)	57.4 (0.8)	274.8 (8.2)	42.6 (0.8)	0.36 (0.04)	–9.93 (2.02)	–0.781 (0.159)
T1107-LA		–	–	355.3 (83.4)	100.0 (0.0)	0.52 (0.08)	–5.78 (1.15)	–0.452 (0.090)
T904	37	6.8 (0.9)	49.0 (7.6)	172.4 (28.8)	51.0 (7.6)	0.46 (0.04)	–6.91 (1.07)	–0.542 (0.054)
T904-LA		5.0 (0.5)	12.6 (8.3)	297.3 (63.6)	87.4 (8.3)	0.73 (0.06)	–5.92 (0.09)	–0.420 (0.084)
F127		24.4 (1.9)	100.0 (0.0)	–	–	0.33 (0.06)	–0.60 (0.10)	–0.058 (0.001)
F127-LA		22.2 (0.3)	88.9 (1.7)	941.4 (24.5)	11.1 (1.7)	0.31 (0.02)	+0.15 (0.00)	+0.006 (0.001)
T1107		17.6 (1.6)	100.0 (0.0)	–	–	0.29 (0.11)	–4.77 (0.81)	–0.458 (0.077)
T1107-LA		14.2 (0.4)	70.1 (8.2)	147.8 (34.6)	29.9 (8.2)	0.28 (0.12)	–6.09 (0.86)	–0.584 (0.068)
T904		12.8 (0.4)	100.0 (0.0)	–	–	0.22 (0.06)	–1.55 (0.70)	–0.149 (0.067)
T904-LA		11.6 (0.9)	63.0 (2.6)	148.2 (37.2)	37.0 (2.6)	0.46 (0.01)	–1.39 (0.17)	–0.133 (0.016)

^a Size population of smaller size

^b Size population of larger size

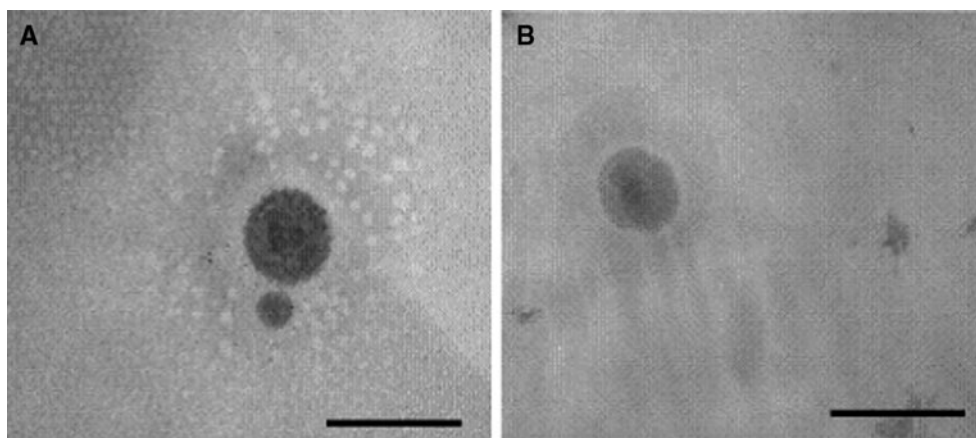


Fig. 7 TEM micrographs of 5 % w/v **A** pristine T904 and **B** T904-LA micelles in water stained with 2 % w/v of uranyl acetate solution. Both samples were stabilized at 37 °C for 30 min prior to the analysis. Scale bar 100 nm

Table 7 Size (D_h) and size distribution (PDI) of 5 % (w/v) pristine and LA-conjugated PEO–PPO block copolymer micelles after incubation in BSA 3 % without and with Con A over 2 h, at 37 °C, as measured by DLS

Copolymer	Con A (mg/mL)	Peak 1 ^a		Peak 2 ^b		PDI (±SD)
		D_h (nm) (±SD)	% Intensity (±SD)	D_h (nm) (±SD)	% Intensity (±SD)	
F127	0	16.1 (0.8)	28.7 (2.1)	167.0 (1.6)	71.3 (2.1)	0.30 (0.07)
	0.5	12.1 (0.6)	22.2 (3.0)	348.8 (28.1)	77.8 (3.0)	0.50 (0.10)
F127-LA	0	17.3 (1.4)	20.3 (0.7)	178.4 (17.4)	79.7 (0.7)	0.20 (0.07)
	0.5	12.8 (2.5)	20.2 (5.8)	479.2 (56.0)*	79.8 (5.8)	0.60 (0.06)
T1107	0	20.0 (2.5)	54.8 (8.7)	225.9 (2.6)	45.2 (8.7)	0.30 (0.05)
	0.5	9.2 (0.2)	21.3 (0.3)	379.2 (25.7)	78.7 (0.3)	0.75 (0.08)
T1107-LA	0	20.5 (2.6)	67.3 (2.3)	238.4 (52.6)	32.7 (2.3)	0.40 (0.20)
	0.5	8.2 (1.9)	12.3 (3.3)	511.4 (85.6)*	87.7 (3.3)	0.79 (0.07)
T904	0	11.4 (0.9)	75.7 (3.0)	207.2 (30.6)	24.3 (3.0)	0.36 (0.04)
	0.5	7.3 (2.6)	67.7 (13.9)	317.0 (109.4)	32.3 (13.9)	0.90 (0.10)
T904-LA	0	12.2 (0.8)	74.9 (1.3)	254.7 (36.5)	25.1 (1.3)	0.40 (0.02)
	0.5	143.8 (40.7)	26.8 (6.1)	503.5 (29.6)*	73.2 (6.1)	0.90 (0.10)

* Statistically significant size increase with respect to the unmodified copolymer treated with Con A ($P < 0.05$)

^a Size population of smaller size

^b Size population of larger size

et al. 2005). Poloxamers and poloxamines were fragmented into fragments of $[m/z]^+$ that fitted well the theoretical molecular weight reported by the supplier and the experimental data determined by gel permeation chromatography divided by two and four (Table 3; Chiappetta et al. 2010). These findings indicated that these copolymers underwent a mild fragmentation. Sosnik et al. (2006) previously analyzed the surface properties of crosslinked poloxamine hydrogels employing a “deep freezing” time-of-flight

secondary ion mass spectrometry technique. However, in that case, the fragmentation was much more profuse and only the molecular weight of the ethylene oxide and propylene oxide units could be detected. Thus, MALDI-TOF MS appeared as a more advantageous methodology. In addition, results showed the increase of the molecular weight upon LA conjugation. On the other hand, the technique was not sensitive enough to reliably quantify the extent of modification as in elemental analysis (Table 2).

The thermal analysis was performed by DSC. The only blocks that could undergo crystallization in PEO–PPOs are those of PEO, while PPO segments are fully amorphous and they display great molecular mobility with a relative low T_g at approximately $-60\text{ }^\circ\text{C}$ (Cohn et al. 2006). Data indicated that T904-LA displayed a dramatic decrease of T_c and a slight decrease of T_m with respect to the pristine counterpart and the highest ΔT of all the lactosylated derivatives; this parameter being calculated to estimate the crystallization tendency (Table 4). These results indicated that the incorporation of LA residues substantially hinders the molecular arrangement of the relatively short PEO segments of T904, leading to a less efficient crystallization. It is worth mentioning that derivative displays the smallest molecular weight (6700 g/mol), the smallest PEO % (40 %) and PEO weight per arm (670 g/mol/arm) and, at the same time, the greatest DLAS (75 %) of all the investigated materials. Thus, this detrimental effect was anticipated. Conversely, F127-LA and T1107-LA showed a slight change of T_c and T_m and a decrease of ΔT that suggested a slightly greater crystallization tendency (Table 4), probably owing to the increased molecular mobility of PEO blocks in presence of LA residues that favoured the rearrangement. A comparison between DSC data of F127 and T1107, two copolymers with similar molecular weight, PEO/PPO relative composition and number of conjugated LA residues though different architecture and thus PEO molecular weight per arm, indicated that F127 was slightly more crystallizable as expressed by the greater values of ΔH_c and ΔH_m . This behavior was related to the fact that in F127 the whole PEO content is divided only into two blocks with molecular weight of approximately 4,410 g/mol, while in T1107 PEO into four of 2,625 g/mol (Gonzalez-Lopez et al. 2008; Alvarez-Lorenzo et al. 2010); PEO blocks of smaller molecular weight usually result in lower T_m and T_c and smaller degree of crystallinity than high molecular weight counterparts (Sosnik and Cohn 2003).

DLS was used to understand effect of LA conjugation on the self-aggregation pattern and the properties of the micelles. Irrespectively of the medium, all the derivatives showed a thermo-responsive behavior characterized by smaller CMC values and micelles of smaller size at $37\text{ }^\circ\text{C}$ than at $25\text{ }^\circ\text{C}$ (Tables 5, 6); a temperature increase leads to the dehydration of PPO blocks and the consequent shrinkage of the micelles

(Cohn et al. 2006). Interestingly, the chemical modification of the amphiphiles resulted in a decrease of the CMC in both water and PBS (Table 5). These findings would suggest that the incorporation of LA residues contributes to the generation of relatively strong H bonds between the terminal hydrophilic blocks that form the micellar corona, this mechanism contributing to physically stabilize the aggregate and to reduce the CMC. Even though previous works indicated that lactosylation slightly enhances the micellization of PEO–PPOs (Li et al. 2009), the extent of the CMC decrease reported in this study is substantially greater.

Poloxamines are pH-dependent molecules and display two pK_a values at 4.0–5.6 and 6.2–8.1 (Gonzalez-Lopez et al. 2008). Thus, depending on the pH of the medium, poloxamine molecules are diprotonated ($\text{pH} < 4$) or monoprotonated ($4 < \text{pH} < 8$) and electrostatic repulsion partially hinders the micellization process. At pH values above 8, poloxamine molecules are unprotonated and micellization is favoured. In other words, poloxamines self-aggregate to a greater extent in more basic pH conditions (Alvarez-Lorenzo et al. 2011). In this context, both T1107 and T904 displayed a smaller CMC in PBS than in water. As it was suggested by different authors, this pH-responsive behavior makes them more versatile biomaterials for drug encapsulation and release applications when compared to the linear counterparts, owing to the ability of modulating the self-assembly pattern under different pH conditions (Gonzalez-Lopez et al. 2008; Chiappetta et al. 2008). Poloxamers show a negligible dependency on the pH. On the other hand, their self-aggregation and gelation strongly depend on the ionic strength and the nature of the ions present in the medium (Chiappetta and Sosnik 2007). In this context, the CMC of F127 and F127-LA was substantially smaller in water than in PBS.

At greater concentrations, PEO–PPO copolymers may display a sol–gel transition upon heating that is characterized by the lower critical solution temperature (LCST) (Cohn et al. 2003, 2005; Sosnik and Cohn 2005). In general, the greater the self-aggregation tendency of the amphiphile (and the lower the CMC), the lower the LCST. LA-conjugated PEO–PPOs could also be envisioned in the development of injectable matrices. However, this study was beyond the scope of this study.

The size, size distribution, and the surface features govern the fate and the performance of the micelles

both in vitro and in vivo. For example, PMs should be small enough to enable administration by the intravenous route, to reduce their recognition by the reticulo-endothelial system cells and to improve their passage across membranes (Chiappetta et al. 2013). Conversely, sufficiently larger micelles are less efficiently filtered by the kidney prolonging the circulation time in plasma. Micelles were thoroughly characterized by DLS at 25 and 37 °C. At 25 °C, LA-conjugated micelles were larger than the pristine ones. At 37 °C, a more complex aggregation pattern was observed. The small-size fraction was smaller than the size of the native copolymer (up to 22.2 nm) due to the thermally induced shrinkage of the micelles (Cohn et al. 2006). In contrast, the larger size fraction resulted in aggregates of substantially larger size (up to 941.4 nm) (Table 6). These findings indicated the secondary aggregation (or fusion) of the micelles and they would suggest that the dehydration of sugar residues is an additional mechanism favouring micellization. At the same time, it is important to stress that sizes were always in the nanometer-size range that allows these polymeric nanocarriers to achieve efficient tissue penetration (Alvarez-Lorenzo et al. 2010).

Complementary TEM analysis indicated that the morphology of the micelles was spherical, sizes being in agreement with DLS analysis (Fig. 7).

Z-pot is a measure of the charge density on the surface of the micelles and it depends on the concentration of the charged moieties and the size of the particle (Chen et al. 2008). A parameter that affects Z-pot is pH. Data clearly indicated that the surface of all the PEO-PPO block copolymers was slightly negatively charged, values ranging between -0.60 and -9.93 mV for pristine copolymers at both tested temperatures (Table 6). Noteworthy, LA-derivatives turned out to be less electronegative than their corresponding counterparts. In addition, the electrophoretic mobility of the modified copolymers fell down with respect to the native ones at both temperatures (Table 6). The reason for the pronounced fall in the electrophoretic mobility would be explained by the chemical modification of the micelle surface with the LA moiety.

Con A exists as a homotetramer at $\text{pH} > 7$ and displays four binding sites (Meng-Xin and Zhi-Kang 2011; Wang et al. 2009; Lu et al. 2006). The binding of Con A to glucose residues takes place through the primary recognition site of Con A, while the secondary

site binding to glucose occurs only optionally (Meng-Xin and Zhi-Kang 2011). Thus, the Con A homotetramer can interact with four glucose units simultaneously. Furthermore, Con A displays specificity for α -D-mannose, α -D-glucose and, to a lesser extent, β -D-glucose with free 3-, 4-, and 6-hydroxyl groups (Meng-Xin and Zhi-Kang 2011; Wang et al. 2009). Con A displays a relatively weak affinity for terminal galactose residues (Wang et al. 2011; Lu et al. 2006). However, LA is galactosylgluconic acid and it comprises a terminal galactose moiety and a non-terminal gluconic acid unit that in the case of LA-conjugated PEO-PPOs is covalently bounded to the copolymer terminal $-\text{OH}$ groups. The gluconic acid unit could be probably recognized by Con A through a secondary site (Meng-Xin and Zhi-Kang 2011; Wang et al. 2009). Thus, even though the outer residue in the conjugates was galactose, the fact that micelles are highly dynamic self-assembly structures could enable the interaction of Con A with gluconic acid as previously suggested (Choi et al. 1998). In this context, the agglutination of LA-conjugated micelles in the presence of Con A was investigated by DLS to assess the ability of the LA-modified micelles to interact with a lectin. The incorporation of BSA ensured the presence of Ca^{2+} ions that are crucial to maintain the lectin as a tetramer (Wang et al. 2011). Measurements showed a non-specific increase in the micellar size of pristine micelles that was probably related to the presence of BSA (Chiappetta et al. 2013). When LA conjugates were analyzed, size growths were more remarkable, indirectly supporting the capacity of the lactosylated amphiphiles to be recognized by lectin-like receptors.

Conclusions

The synthesis of LA-modified linear and branched PEO-PPO block copolymers was investigated and the products thoroughly characterized. Elemental analysis indicated the incorporation of one LA unit per F127 and T1107 molecule and three for T904. These results with those obtained using $^1\text{H-NMR}$, $^{13}\text{C-NMR}$, ATR/FT-IR, and MALDI-TOF MS confirmed the structure of the different conjugates. The conjugation of LA moieties favored the micellization process, as expressed by the lower CMC values measured, and would increase their physical stability upon dilution.

This performance would represent an additional advantageous feature of these derivatives toward the encapsulation and targeting of drugs. Finally, Con A experiments strongly suggested that LA-conjugated micelles could be recognized by the ASGPRs present on the surface of hepatocytes. Current studies are being devoted to explore the capacity of these modified nanocarriers to encapsulate and target drugs to liver cells.

Acknowledgments MLC, VM, and AS are staff members of CONICET. R Glisoni thanks the postdoctoral scholarship of CONICET. This study was supported by research Grants from University of Buenos Aires (UBACYT 20020090200016) and CONICET (Grant PIP 0220). The authors are very thankful to Prof. Dr. Carmen Alvarez-Lorenzo (Department of Pharmacy and Pharmaceutical Technology, Universidad de Santiago de Compostela, Santiago de Compostela, Spain) and Prof. Dr. Viviana Campo Campo Dall'Orto (Department of Analytical Chemistry, Faculty of Pharmacy and Biochemistry, University of Buenos Aires) for the use of DSC and MALDI-TOF mass spectroscopy and ATR/FT-IR equipment, respectively.

References

- Alvarez-Lorenzo C, Rey-Rico A, Brea J, Loza MI, Concheiro A, Sosnik A (2010) Inhibition of P-glycoprotein pumps by PEO-PPO amphiphiles: branched versus linear derivatives. *Nanomedicine (Lond.)* 5:1571–1583
- Alvarez-Lorenzo C, Sosnik A, Concheiro A (2011) PEO-PPO block copolymers for passive micellar targeting and overcoming multidrug resistance in cancer therapy. *Curr Drug Targets* 12:1112–1130
- Boetz A, Russ T, Gores F, Karas M, Kreuter J (2005) Molecular weights of poly(butyl cyanoacrylate) nanoparticles determined by mass spectrometry and size exclusion chromatography. *Eur J Pharm Biopharm* 60:391–399
- Casali M, Riva S, Ferruti P (2001) Use of new aminosugar derivatives as co-monomers for the synthesis of glycosylated poly(amido-amines). *J Bioact Comp Polym* 16:479–491
- Chen Y, Cui G, Zhao M, Wang C, Qian K, Morris-Natsche S, Lee KH, Peng S (2008) Synthesis, nano-scale assembly, and in vivo anti-thrombotic activity of novel short peptides containing L-Arg and L-Asp or L-Glu. *Bioorg Med Chem* 16:5914–5925
- Chiappetta DA, Sosnik A (2007) Poly(ethylene oxide)-poly(propylene oxide) block copolymer micelles as drug delivery agents: improved hydrosolubility, stability and bioavailability of drugs. *Eur J Pharm Biopharm* 66:303–317
- Chiappetta DA, Degrossi J, Teves S, D'Aquino M, Bregni C, Sosnik A (2008) Triclosan-loaded poloxamine micelles for enhanced antibacterial activity against biofilm. *Eur J Pharm Biopharm* 69:535–545
- Chiappetta DA, Alvarez-Lorenzo C, Rey-Rico A, Taboada P, Concheiro A, Sosnik A (2010) N-alkylation of poloxamines modulates micellar encapsulation and release of the antiretroviral efavirenz. *Eur J Pharm Biopharm* 76:24–37
- Chiappetta DA, Facorro G, Rubin de Celis E, Sosnik A (2011) Synergistic encapsulation of the anti-HIV agent efavirenz within mixed poloxamine/poloxamer polymeric micelles. *Nanomedicine: NBM* 7:624–637
- Chiappetta DA, Hocht C, Opezco JAW, Sosnik A (2013) Intranasal administration of antiretroviral-loaded micelles for anatomical targeting to the brain in HIV. *Nanomedicine (Lond.)* 1–15
- Choi YH, Liu F, Park JS, Kim SW (1998) Lactose-poly(ethylene glycol)-grafted poly-L-lysine as hepatoma cell-targeted gene carrier. *Bioconj Chem* 9:708–718
- Cohn D, Sosnik A, Levy A (2003) Improved reverse thermoresponsive polymeric systems. *Biomaterials* 24:3707–3714
- Cohn D, Sosnik A, Garty S (2005) Smart hydrogels for in situ-generated implants. *Biomacromolecules* 6:1168–1175
- Cohn D, Lando G, Sosnik A, Garty S, Levi A (2006) Novel degradable reverse thermoresponsive multiblock copolymers. *Biomaterials* 27:1718–1727
- Cuestas ML, Mathet VL, Oubiña JR, Sosnik A (2010) Drug delivery systems and liver targeting for the improved pharmacotherapy of the hepatitis B virus (HBV) infection. *Pharm Res* 27:1184–1202
- De Paula D, Bentley VLB, Mahato RI (2007) Hydrophobization and bioconjugation for enhanced siRNA delivery and targeting. *RNA* 13:431–456
- Eisenburg C, Seta N, Appel M, Feldmann G, Durand G, Feger J (1991) Asialoglycoprotein receptor in human isolated hepatocytes from normal liver and its apparent increase in liver with histological alterations. *J Hepatol* 13:305–309
- El-Seraq HB, Rudolph KL (2007) Hepatocellular carcinoma: epidemiology and molecular carcinogenesis. *Gastroenterology* 132:2557–2576
- Enrich C, Verges M, Evans WH (1992) Differential expression of asialoglycoprotein receptor subunits in the endocytic compartment during liver regeneration. *J Cell Physiol* 150:344–352
- Eto T, Takahashi H (1999) Enhanced inhibition of hepatitis B virus production by asialoglycoprotein receptor-directed interferon. *Nat Med* 5:577–581
- Feng M, Cai Q, Shi X, Huang H, Zhou P, Guo X (2008) Recombinant high-density lipoprotein complex as targeting system of nosiheptide to liver cells. *J Drug Target* 16:502–508
- Fernandez-Tarrio M, Alvarez-Lorenzo C, Concheiro A (2007) Calorimetric approach to Tetronic/water interactions. *J Therm Anal Calorim* 87:171–178
- Fiume L, Busi C, Di Stefano G, Mattioli A (1994) Targeting of antiviral drugs to the liver using glycoprotein carriers. *Adv Drug Del Rev* 14:51–65
- Gallet G, Carroccio S, Rizzarelli P, Karlsson S (2002) Thermal degradation of poly(ethylene oxide-propylene oxide-ethylene oxide) triblock copolymer: comparative study by SEC/NMR, SEC/MALDI-TOF-MS and SPME/GC-MS. *Polymer* 43:1081–1094
- Gao S, Chen J, Xu X, Ding Z, Yang Y-H, Hua Z, Zhang J (2003) Galactosylated low molecular weight chitosan as DNA carrier for hepatocyte-targeting. *Int J Pharm* 255:57–68
- Giacomelli C, Schmidt V, Borsali R (2007) Nanocontainers formed by self-assembly of poly(ethylene oxide)-*b*-poly(glycerol monomethacrylate)-drug conjugates. *Macromolecules* 40:2148–2157

- Glisoni RJ, Chiappetta DA, Finkielstein LM, Moglioni AG, Sosnik A (2010) Self-aggregation behaviour of novel thiosemicarbazone drug candidates with potential antiviral activity. *New J Chem* 34:2047–2058
- Glisoni RJ, Chiappetta DA, Moglioni AG, Sosnik A (2012a) Novel 1-indanone thiosemicarbazone antiviral candidates: aqueous solubilization and physical stabilization by means of cyclodextrins. *Pharm Res* 29:739–755
- Glisoni RJ, Cuestas ML, Mathet V, Oubiña J, Moglioni AG, Sosnik A (2012b) Antiviral activity against the hepatitis C virus (HCV) of 1-indanone thiosemicarbazones and their inclusion complexes with hydroxypropyl- β -cyclodextrin. *Eur J Pharm Sci* 47:596–603
- Gonzalez-Lopez J, Alvarez-Lorenzo C, Taboada P, Sosnik A, Sandez-Macho I, Concheiro A (2008) Self-associative behavior and drug-solubilizing ability of poloxamine (tetronic) block copolymers. *Langmuir* 24:10688–10697
- Guidotti LG, Chisari FV (2006) Immunobiology and pathogenesis of viral hepatitis. *Annu Rev Pathol Mech Dis* 1:23–61
- Gupta U, Jain NK (2010) Non-polymeric nano-carriers in HIV/AIDS drug delivery and targeting. *Adv Drug Deliv Rev* 62:478–490
- Kataoka K, Harada A, Nagasaki Y (2001) Block copolymer micelles for drug delivery: design, characterization and biological significance. *Adv Drug Deliv Rev* 47:113–131
- Kikker R, Lepenies B, Dibekian A, Laurino P, Seeberger PH (2009) In vitro imaging and in vivo liver targeting with carbohydrate capped quantum dots. *J Am Chem Soc* 131:2110–2112
- Kim TH, Park IK, Nah JW (2004) Galactosylated chitosan/DNA nanoparticles prepared using water-soluble chitosan as a gene carrier. *Biomaterials* 25:3783–3792
- Kim SI, Shin D, Lee H, Ahn BY, Yoon Y, Kim M (2009) Targeted delivery of siRNA against hepatitis C virus by apolipoprotein A-I-bound cationic liposomes. *J Hepatol* 50:479–488
- Li Y, Huang G, Diakur J, Wiebe LI (2008) Targeted delivery of macromolecular drugs: asialoglycoprotein receptor (AS-PGR) expression by selected hepatoma cell lines used in antiviral drug development. *Curr Drug Deliv* 5:299–302
- Li X, Huang Y, Chen X, Zhou Y, Zhang Y, Li P, Liu Y, Sun Y, Zhao J, Wang F (2009) Self-assembly and characterization of Pluronic P105 micelles for liver-targeted delivery of silybin. *J Drug Target* 17:739–750
- Li Y, Hoskins JN, Sreerama SG, Grayson MA, Grayson SM (2010) The identification of synthetic homopolymer end groups and verification of their transformations using MALDI-TOF mass spectrometry. *J Mass Spectrom* 45:587–611
- Lu C, Chen X, Xie Z, Lu T, Wang X, Ma J, Jing X (2006) Biodegradable amphiphilic triblock copolymer bearing pendant glucose residues: preparation and specific interaction with concanavalin A molecules. *Biomacromolecules* 7:1806–1810
- Mao SJ, Bi YQ, Jin H, Wei DP, He R, Hou SX (2007) Preparation, characterization and uptake by primary cultured rat hepatocytes of liposomes surface-modified with glycyrrhithinic acid. *Pharmazi* 62:614–619
- Meng-Xin H, Zhi-Kang X (2011) Carbohydrate decoration of microporous polypropylene membranes for lectin affinity adsorption: comparison of mono- and disaccharides. *Colloids Surf B* 85:19–25
- Nishina K, Unno T, Uno Y, Kubodera T, Kanouchi T, Mizusawa H, Yokota T (2008) Efficient in vivo delivery of siRNA to the liver by conjugation of α -tocopherol. *Mol Ther* 16:734–740
- Raith K, Schmelzer CEH, Neubert RHH (2006) Towards a molecular characterization of pharmaceutical excipients: mass spectrometric studies of ethoxylated surfactants. *Int J Pharm* 319:1–12
- Sato Y, Murase K, Kato J, Kobune M, Sato T, Kawano Y, Takimoto R, Takada K, Miyanishi K, Matsunaga T, Takayama T, Niitsu Y (2008) Resolution of liver cirrhosis using vitamin A-coupled liposomes to deliver siRNA against a collagen-specific chaperone. *Nat Biotechnol* 26:431–442
- Sosnik A, Cohn D (2003) Poly(ethylene glycol)-poly(epsilon-caprolactone) block oligomers as injectable materials. *Polymer* 44:7033–7042
- Sosnik A, Cohn D (2005) Reverse thermo-responsive poly(ethylene oxide) and poly(propylene oxide) multi-block copolymers. *Biomaterials* 26:349–357
- Sosnik A, Sefton MV (2006) Methylation of poloxamine for enhanced cell adhesion. *Biomacromolecules* 7:331–338
- Sosnik A, Brodersen P, Sodhi RNS, Sefton MV (2006) Surface study of collagen/poloxamine hydrogels by a 'deep freezing' ToF-SIMS approach. *Biomaterials* 27:2340–2348
- Sosnik A, Carcaboso A, Chiappetta DA (2008) Polymeric nanocarriers: new endeavors for the optimization of the technological aspects of drugs. *Recent Pat Biomed Eng* 1:43–59
- Tozawa R, Ishibashi S, Osuga J, Yamamoto K, Yagyu H, Ohashi K, Tamura Y, Yahagi N, Iizuka Y, Okazaki H, Harada K, Gotoda T, Shimano H, Kimura S, Nagai R, Yamada N (2001) Asialoglycoprotein receptor deficiency in mice lacking the major receptor subunit. Its obligate requirement for the stable expression of oligomeric receptor. *J Biol Chem* 276:12624–12628
- Trevaskis NL, Charman WN, Porter CJH (2010) Targeted drug delivery to lymphocytes: a route to site-specific immunomodulation? *Mol Pharm* 7:2297–2309
- Vetri V, Carrotta R, Picone P, Di Carlo M, Militello V (2010) Concanavalin A aggregation and toxicity on cell cultures. *Biochim Biophys Acta* 1804:173–183
- Wang S, Deng Y, Xu H (2006) Synthesis of a novel galactosylated lipid and its application to the hepatocyte-selective targeting of liposome doxorubicin. *Eur J Pharm Biopharm* 62:32–38
- Wang Z, Yuan Z, Jin L (2008) Gene delivery into hepatocytes with the preS/liposome/DNA system. *Biotechnol J* 3:1286–1295
- Wang X, Liu LH, Ramström O, Yan M (2009) Engineering nanomaterial surfaces for biomedical applications. *Exp Biol Med* 234:1128–1139
- Wang X, Ramström O, Yan M (2011) Dynamic light scattering as an efficient tool to study glyconanoparticle-lectin interactions. *Analyst* 136:4174–4178
- Weeke-Klimp AH, Bartsch M, Morselt HW, Van Veen-Hof I, Meijer DK, Scherphof GL, Kamps JA (2007) Targeting of stabilized plasmid lipid particles to hepatocytes in vivo by means of coupled lactoferrin. *J Drug Target* 15:585–594

- Wu GY, Wu CH (1998) Receptor mediated delivery of foreign genes to hepatocytes. *Adv Drug Deliv Rev* 29:243–248
- Yang J, Bo XC, Ding XR, Dai JM, Zhang ML, Wang XH, Wang SQ (2006) Antisense oligonucleotides targeted against asialoglycoprotein receptor 1 block human hepatitis B virus replication. *J Viral Hepat* 13:158–165
- Zhang J, Li C, Cheng HW, Xue ZY, Huang FW, Zhuo RX, Zhang XZ (2011) Fabrication of lactobionic-loaded chitosan microcapsules as potential drug carriers targeting the liver. *Acta Biomater* 7:1655–1673